



1 Composition and light absorption of nitroaromatic compounds in  
2 organic aerosols from laboratory biomass burning

3

4 Mingjie Xie<sup>1,2,3,4,\*</sup>, Xi Chen<sup>4</sup>, Michael D. Hays<sup>4</sup>, Amara L. Holder<sup>4</sup>

5

6 <sup>1</sup>Collaborative Innovation Center of Atmospheric Environment and Equipment Technology,  
7 Jiangsu Key Laboratory of Atmospheric Environment Monitoring and Pollution Control, School  
8 of Environmental Science and Engineering, Nanjing University of Information Science &  
9 Technology, 219 Ningliu Road, Nanjing 210044, China

10 <sup>2</sup>State Key Laboratory of Pollution Control and Resource Reuse, School of the Environment,  
11 Nanjing University, Nanjing, China

12 <sup>3</sup>Oak Ridge Institute for Science and Education (ORISE), Office of Research and Development,  
13 U.S. Environmental Protection Agency, 109 T.W. Alexander Drive, Research Triangle Park, NC  
14 27711, USA

15 <sup>4</sup>National Risk Management Research Laboratory, Office of Research and Development, U.S.  
16 Environmental Protection Agency, 109 T.W. Alexander Drive, Research Triangle Park, NC  
17 27711, USA

18

19

20 \*Correspondence to: Mingjie Xie

21 E-mail: [mingjie.xie@colorado.edu](mailto:mingjie.xie@colorado.edu); [mingjie.xie@nuist.edu.cn](mailto:mingjie.xie@nuist.edu.cn);

22 Tel: +86-18851903788;

23 Fax: +86-25-58731051;

24 Mailing address: 219 Ningliu Road, Nanjing, Jiangsu, 210044, China

25

26

27

28

29

30 **ABSTRACT**

31 This study seeks to understand the compositional details of nitroaromatic compounds  
32 (NACs) emitted during biomass burning (BB) and their contribution to light-absorbing organic  
33 carbon (OC), also termed brown carbon (BrC). Three laboratory BB experiments were conducted  
34 with two U.S. pine forest understory fuels typical of those consumed during prescribed fires.  
35 During the experiments, submicron aerosol particles were collected on filter media and  
36 subsequently extracted with methanol and examined for their optical and chemical properties.  
37 Significant correlations ( $p < 0.05$ ) were observed between BrC absorption and elemental carbon  
38 (EC)/OC ratios for test specific data. However, the pooled experimental data indicated that the  
39 BB BrC absorption depends on more than the BB fire conditions as represented by the EC/OC  
40 ratio. Fourteen NACs were identified in the BB samples, four of which ( $C_{10}H_{11}NO_4$ ,  $C_{10}H_{11}NO_5$ ,  
41  $C_{11}H_{13}NO_5$  and  $C_{11}H_{13}NO_6$ ) have not been observed previously in chamber-based secondary  
42 organic aerosols, and are expected to have methoxyphenol-type structure specific to the  
43 pyrolyzed biomass lignin based on mass spectral evidence, suggesting these compounds may be  
44 unique to BB aerosols. The average total contribution of NACs to organic mass ( $0.023 \pm 0.0089$   
45 to  $0.18 \pm 0.067\%$ ) was 5–10 times lower than the average contribution to the overall BrC  
46 absorption at 365 nm ( $0.12 \pm 0.047$  to  $2.44 \pm 0.67\%$ ). The average contributions (%) of total  
47 NACs to organic mass and aqueous extracts absorption correlated significantly ( $p < 0.05$ ) with  
48 EC/OC for both test specific and pooled experimental data. These results suggested that the  
49 formation of NACs from BB depended more on burn conditions than the bulk absorptive  
50 properties of BB BrC.

51

52



## 53 **1 Introduction**

54 Biomass burning (BB), including residential burning for cooking, heating, and open  
55 burning, is a major source of atmospheric carbonaceous aerosol, contributing 62% and 93% of  
56 black carbon (BC) and primary organic carbon (OC) emissions, respectively (Bond et al., 2004).  
57 BC can absorb sunlight across the entire spectral range with a weak dependence on wavelength  
58 ( $\lambda$ ) (Bond, 2001; Bond et al., 2013; Lack and Langridge, 2013), while light absorption of BB OC  
59 increases rapidly from the shorter visible region (400–550 nm) to the ultraviolet (UV) region  
60 (300–400 nm) (Kirchstetter et al., 2004; Laskin et al., 2015; Chakrabarty et al., 2016; Xie et al.,  
61 2017b). The light absorption caused by BC and OC from BB can affect the Earth's radiative  
62 balance (Ramanathan et al., 2001; Anderson et al., 2003; Bond and Bergstrom, 2006), and BC  
63 emission factors and its warming effect have been intensively investigated (Bond et al.,  
64 2004; Bond et al., 2013). However, the optical properties and chemical composition of light-  
65 absorbing OC, also termed brown carbon (BrC) from BB is less well characterized. The  
66 chromophores in BrC are expected to have high degree of unsaturation or conjugation (Chen and  
67 Bond, 2010; Lin et al., 2014; Laskin et al., 2015), but are seldom identified and used as BrC  
68 tracers in the atmosphere (Desyaterik et al., 2013; Zhang et al., 2013; Teich et al., 2016).

69 Polycyclic aromatic hydrocarbons (PAHs) and their derivatives are typical BrC  
70 chromophores (Samburova et al., 2016; Huang et al., 2018), of which the light absorption in the  
71 UV and visible wavelength range is highly dependent on ring numbers and degree of conjugation  
72 (Samburova et al., 2016). However, PAH emissions are not source-specific, but are associated  
73 with multiple different combustion processes, including BB (Samburova et al., 2016), coal  
74 burning (Chen et al., 2005), motor vehicle emissions (Riddle et al., 2007), etc. Therefore, PAHs  
75 are not unique to BB BrC. Nitroaromatic compounds (NACs) are another class of BrC



76 chromophores that have been detected in BB (Lin et al., 2016), cloud water (Desyaterik et al.,  
77 2013) and atmospheric particles (Zhang et al., 2013;Teich et al., 2017). In water extracts of  
78 atmospheric particles, NACs contribute greater than 3% of the light absorption at 365–370 nm  
79 (Zhang et al., 2013;Teich et al., 2016). Lin et al. (2017) investigated the influence of BB on BrC  
80 absorption during a nationwide bonfire festival in Israel, and found that NACs accounted for 50%  
81 – 80% of water extractable BrC absorption at  $\lambda > 400$  nm. These results suggest that NACs are  
82 important BB BrC chromophores, but their composition and structures are less certain.  
83 Nitrophenols, nitrocatechols, and methyl nitrocatechols (including isomers) are commonly  
84 observed in BB aerosols (Claeys et al., 2012;Lin et al., 2016;Lin et al., 2017), and are also  
85 generated from the photo-oxidation of benzene, toluene, and *m*-creosol in the presence of NO<sub>x</sub>  
86 (Iinuma et al., 2010;Lin et al., 2015;Xie et al., 2017a). As such, other NAC structures specific to  
87 BB are needed to represent BB BrC chromophores. Additionally, very few studies have  
88 examined the influence of burn conditions on the formation of NACs in BB emissions, although  
89 it is well known that increasing combustion temperature, or flaming dominated combustion, is  
90 associated with strong BrC absorption (Chen and Bond, 2010;Saleh et al., 2014).

91 The present study attempts to identify additional NAC structures in laboratory BB  
92 samples, characterize the compositional profile of NACs from BB, and investigate the  
93 relationship between their formation and fire conditions. A high-performance liquid  
94 chromatograph interfaced to a diode array detector (HPLC/DAD) and quadrupole (Q)-time-of-  
95 flight mass spectrometer (ToF-MS) was used to examine NACs in PM<sub>2.5</sub> (particulate matter with  
96 aerodynamic diameter  $\leq 2.5$   $\mu\text{m}$ ) from three BB experiments. A thermal-optical instrument  
97 determined bulk OC and elemental carbon (EC) in the PM, and a UV/Vis spectrometer was used  
98 to measure total BrC absorption in methanol extracts of BB PM<sub>2.5</sub>. The results of this study will



99 benefit the exploration of organic molecular markers for BB BrC in the atmosphere, and help  
100 explain the influence of fire conditions on the formation of BrC chromophores.

## 101 **2 Methods**

### 102 **2.1 Laboratory open BB simulations**

103 Laboratory simulations of open BB were conducted at the U.S. EPA [Research Triangle  
104 Park (RTP), North Carolina (NC)] Open Burn Test Facility (OBTF), a 70 m<sup>3</sup> enclosure, as  
105 detailed in Grandesso et al. (2011). Details of the protocols for biomass fuel collection and burn  
106 simulations were provided elsewhere (Aurell and Gullett, 2013; Aurell et al., 2015; Holder et al.,  
107 2016). Briefly, forest understory fuels were gathered from two different locations in the  
108 southeastern United States — Florida (FL) and NC. The FL forest field (Eglin Air Force Base,  
109 FL) is characteristic of a well-managed long leaf pine (*Pinus palustris*) ecosystem. The NC  
110 forest was located near the EPA campus in RTP, and it contained mainly Loblolly pine (*Pinus*  
111 *taeda*) with some deciduous hardwood trees leaf litter. Biomass fuel was divided by a quartering  
112 procedure (Aurell and Gullett, 2013) and burned in batches (1 kg) on an aluminum foil-coated  
113 steel pan (1 m × 1 m). Ambient air was pulled into the OBTF through a large inlet at ground  
114 level and the combustion exhaust was drawn through a roof duct near a baghouse using a high-  
115 volume blower. PM<sub>2.5</sub> was sampled at 10 L min<sup>-1</sup> on Teflon (47 mm, Pall, Ann Arbor, Michigan,  
116 USA) and pre-heated (550 °C, 12 h) quartz filters (QF, diameter 43 mm, Pall) with a PM<sub>2.5</sub>  
117 impactor (SKC, Pittsburgh, Pennsylvania, USA). For the NC forest fire simulation, filter samples  
118 were collected during an initial flaming phase lasting approximately 1–3 minutes. After most of  
119 the flames were extinguished, a second set of filter samples were obtained for the smoldering  
120 emissions. Smoldering samples were collected until there was little or no visible smoke being  
121 emitted from the fuel bed, typically lasting 6–15 minutes. Two separate experiments were done



122 with the NC forest fuels in spring and summer, respectively, with different ambient temperatures  
123 (Table S1). Sampling of the FL forest fire simulations was done in autumn over the complete  
124 burn, not by combustion phase. Only one experiment was done for the FL forest fuels collected  
125 in fall. Background samples were obtained post-burn inside the OBTF. A summary of the sample  
126 information is provided in Table S1 of the supporting information.

## 127 **2.2 Bulk carbon and light absorption measurement**

128 Details of the bulk OC, EC and light absorption analysis methods are provided in Xie et  
129 al. (2017a,b). Briefly, the bulk OC and EC were measured using an OC-EC analyzer (Sunset  
130 Laboratories, Portland, OR) with a modified NIOSH method 5040 protocol (NIOSH, 1999).  
131 Filters were extracted in methanol (supplementary information) and the light absorption of the  
132 extracts was measured by a UV/Vis spectrometer (V660, Jasco Incorporated, Easton MD). The  
133 extraction efficiency ( $\eta$ , %) was calculated from the analysis of residual OC on the methanol-  
134 extracted filter. The light absorption coefficient ( $Abs_{\lambda}$ ,  $Mm^{-1}$ ), mass absorption coefficient  
135 ( $MAC_{\lambda}$ ,  $m^2 gC^{-1}$ ) and solution absorption Ångström exponent ( $\hat{A}_{abs}$ ) of methanol extractable OC  
136 were calculated to reflect the light-absorbing properties of bulk BB BrC. Details of the  
137 calculation method are provided in the supplementary information. In this work, we focus on the  
138 BrC absorption at  $\lambda = 365$  and  $550$  nm, representing near UV and visible regions (Zhang et al.,  
139 2013; Saleh et al., 2014), respectively.

## 140 **2.3 Filter extraction and HPLC/DAD-Q-ToFMS analysis**

141 The  $PM_{2.5}$  filter extraction and subsequent instrumental analysis methods used here are  
142 the same as those described in Xie et al. (2017a). Briefly, a  $4-6$   $cm^2$  piece of each filter was pre-  
143 spiked with  $25$   $\mu L$  of  $10$   $ng \mu L^{-1}$  nitrophenol-d4 (internal standard, IS), and extracted  
144 ultrasonically in  $3-5$  mL of methanol twice (15 min each). After filtration and concentration, the



145 final volume was roughly 500  $\mu\text{L}$  prior to HPLC/DAD-Q-ToFMS analysis. An Agilent 1200  
146 series HPLC equipped with a Zorbax Eclipse Plus C18 column (2.1 $\times$ 100 mm, 1.8  $\mu\text{m}$  particle  
147 size, Agilent Technologies) was used to separate the target NACs; the identification and  
148 quantification of NACs were determined with an Agilent 6520 Q-ToFMS. The Q-ToFMS was  
149 equipped with a multimode ion source operating in electrospray ionization (ESI) and negative ( $-$ )  
150 ion modes. All samples were analyzed in full scan mode (40–1000 Da), and then selected  
151 samples were re-examined using MS/MS mode under identical chromatographic conditions. The  
152 MS/MS spectra of target  $[\text{M}-\text{H}]^-$  ions provided  $m/z$  data, which was used for identifying NAC  
153 structures. Table S2 provides the standard, surrogate assignments, proposed structures, and  
154 formulas of the identified NACs. The criterion for surrogate selection is provided in  
155 supplementary information. Acceptance criterion of  $\pm 10$  ppm mass accuracy was set for  
156 compound identification and quantification. The extracted ion chromatograms (EICs) and Q-ToF  
157 MS/MS spectra for identified compounds in selected BB samples are provided in Figs. S1–S2 of  
158 the supplementary information. The Q-ToF MS/MS spectra of standard or surrogate compounds  
159 used in this work are provided in Fig. S3 for comparison. The quality assurance and quality  
160 control (QA/QC) procedures applied for NACs quantification were provided in Xie et al. (2017a).  
161 Quantification was conducted using the internal standard method with 9-point calibration curves  
162 ( $\sim 0.01$ – $2$  ng  $\mu\text{L}^{-1}$ ). The compounds corresponding to each NAC formula (including isomers)  
163 were quantified individually and added together for the calculation of mass contribution (%) to  
164 organic matter (OM  $\mu\text{g m}^{-3}$ ) in each sample. Field blank and background samples were free of  
165 contamination for NACs. Average recoveries of standard compounds ranged from 75.1 to 116%,  
166 and the method detection limit ranged from 0.70 to 17.6 pg (Table S3).

### 167 **3 Results and discussion**



### 168 3.1 Light absorption of extractable OC

169 The average EC/OC ratio, OC extraction efficiency,  $MAC_{365}$ ,  $MAC_{550}$ , and  $\dot{A}_{abs}$  of all  
170 samples grouped by experiment and fire phase are shown in Table 1. Abbreviations for each  
171 sample group are also listed in the table. The optical properties and bulk composition of the FL  
172 forest samples were reported in Xie et al. (2017b). The average extraction efficiency for all  
173 groups of BB samples is greater than 95% (range  $97.0 \pm 1.87$  to  $99.5 \pm 0.33\%$ ), and the light  
174 absorption exhibits strong wavelength dependence, with average  $\dot{A}_{abs}$  values ranging from  $5.68 \pm$   
175  $0.70$  to  $7.95 \pm 0.22$ . For each of the two NC forest experiments, the samples collected during the  
176 flaming phase (NF1 and NF2) have significantly higher (student's  $t$  test,  $p < 0.05$ ) average  
177 EC/OC ratios,  $MAC_{365}$  and  $MAC_{550}$ , and lower ( $p < 0.05$ )  $\dot{A}_{abs}$  than those collected during the  
178 smoldering phase (NS1 and NS2). When combining the results from the two NC forest  
179 experiments, the average  $MAC_{365}$  values for NC forest 2 are significantly ( $p < 0.05$ ) higher than  
180 NC forest 1, despite having a comparable EC/OC ratio (NF1 =  $0.042 \pm 0.014$  and NF2 =  $0.049 \pm$   
181  $0.011$ , NS1 =  $0.0098 \pm 0.0024$  and NS2 =  $0.0075 \pm 0.0026$ ). Additionally, the average EC/OC  
182 ratio of FF samples is 5–30 times higher than NF and NS samples, while the average  $MAC_{365}$   
183 and  $MAC_{550}$  values of FF samples ( $1.13 \pm 0.15$  and  $0.053 \pm 0.023 \text{ m}^2 \text{ gC}^{-1}$ ) are comparable to  
184 NS1 samples ( $1.10 \pm 0.11$  and  $0.054 \pm 0.015 \text{ m}^2 \text{ gC}^{-1}$ ), but lower than other NC forest samples.

185 High temperature pyrolysis or intense flaming conditions are known to increase the  
186 fraction of EC in the total carbonaceous aerosol emissions of BB (Hosseini et al., 2013; Eriksson  
187 et al., 2014; Martinsson et al., 2015; Nielsen et al., 2017). Several studies found that the light-  
188 absorbing properties of BB OC could be parameterized as a function of the EC/OC or  
189 BC/organic aerosol (OA) ratio, a measurement proxy for burn conditions (McMeeking et al.,  
190 2014; Saleh et al., 2014; Lu et al., 2015; Pokhrel et al., 2016), and inferred that the absorptivity of





191 BB OC depended strongly on burn conditions, not fuel type. In Xie et al. (2017b), significant  
192 correlations ( $p < 0.05$ ) between  $MAC_{365}$  of methanol extractable OC from BB and EC/OC ratios  
193 were observed only for samples with identical fuel type, but not for pooled samples with  
194 different fuel types, indicating that both burn conditions and fuel types can impact the light  
195 absorption of BB OC. The contradiction is possibly ascribed to different approaches used in  
196 characterizing the light absorption of BB OC and different test fuel types (Xie et al., 2017b).

197 In this work, the comparison of the flaming versus smoldering samples for each NC  
198 experiment suggests that the light absorption of OC from BB is strongly dependent on burn  
199 conditions when the fuel type and ambient conditions are similar. The difference in  $MAC_{365}$   
200 values between the two NC forest experiments might suggest that the light absorption of BB OC  
201 is also dependent on ambient conditions, as the two NC forest experiments were conducted in  
202 spring and summer, respectively, with distinct ambient conditions (Table S1). The comparison of  
203 the FL versus NC forest experiments suggests that the fuel type can also play a role in BB OC  
204 absorption. Thus, the light absorption of BB OC may be influenced by factors other than burn  
205 conditions. Additionally, EC/OC ratios alone may not predict BB OC light absorption from  
206 burns with varying fuel types and ambient conditions.

### 207 **3.2 Identification and quantification of NACs**

208 In the current work, fourteen NAC chemical formulas in BB samples were identified  
209 (Table S2) using the HPLC/DAD-Q-ToFMS analysis, covering all the NACs with high  
210 abundance and strong absorption in ambient and BB particles reported in previous work (Claeys  
211 et al., 2012; Mohr et al., 2013; Zhang et al., 2013; Chow et al., 2016; Lin et al., 2016; Lin et al.,  
212 2017). Their EICs are provided in Fig. S1. The NACs structures corresponding to each chemical  
213 formula were examined using MS/MS data in Fig. S2. In Table S4, the averages and ranges of



214 relative mass contribution of identified NACs to OM are provided by BB experiment and burn  
215 condition. Here the OM mass was calculated as  $1.7 \times \text{OC mass}$  (Turpin et al, 2001). In addition,  
216 the average relative mass contributions of each NAC in BB samples are shown in Fig. 1.

217 The three BB experiments have consistent mass contribution profiles (Fig. 1), although  
218 they used different fuel types and were conducted in different seasons. The BB samples collected  
219 during flaming periods (NF1 and NF2) contain significantly higher ( $p < 0.05$ ) average relative  
220 mass contributions from total NACs to OM ( $t\text{NAC}_{\text{OM}}\%$ : NF1  $0.18 \pm 0.067\%$ , NF2  $0.16 \pm$   
221  $0.045\%$ ) than those collected during smoldering periods (NS1  $0.055 \pm 0.026\%$ , NS2  $0.023 \pm$   
222  $0.0089\%$ ). During the FL forest burn experiment, flaming and smoldering phases were not  
223 separated for sampling, and the average  $t\text{NAC}_{\text{OM}}\%$  is  $0.13 \pm 0.059\%$ , which is between the  
224  $t\text{NAC}_{\text{OM}}\%$  of the flaming and smoldering samples of the NC forest experiments. If we  
225 recalculate the average  $t\text{NAC}_{\text{OM}}\%$  for the NC forest experiments by combining the flaming and  
226 smoldering sample data in each burn, the three BB experiments (FL forest, NC forest 1 and 2)  
227 show similar average  $t\text{NAC}_{\text{OM}}\%$  ( $0.11 \pm 0.017$ – $0.13 \pm 0.059\%$ ), and the average  $t\text{NAC}_{\text{OM}}\%$   
228 across all samples in this work is  $0.12 \pm 0.051\%$  (range 0.037 to 0.21%). This value is  
229 comparable to that observed at Detling ( $\sim 0.5\%$ ), United Kingdom during winter, when domestic  
230 wood burning is prevalent (Mohr et al., 2013). In the current work, most of the NACs were  
231 quantified using surrogates, and their contributions to OM from BB may change if authentic  
232 standards or different surrogates are used for quantification. However, the three experiments  
233 might still have consistent relative mass contribution profiles of NACs and similar average  
234  $t\text{NAC}_{\text{OM}}\%$ , assuming burn conditions and fuel types have minor impact on the OM/OC ratio.  
235 Therefore, unlike the light absorption of methanol extractable OC, the formation of NACs in BB  
236 seem to depend largely on burn conditions, rather than fuel types and ambient conditions.



237           Among the fourteen identified NAC formulas,  $C_6H_5NO_4$  and  $C_9H_9NO_4$  have the highest  
238 concentrations (Fig. 1) in FL forest and NC forest flaming-phase samples, accounting for  $0.029 \pm$   
239  $0.011$  to  $0.037 \pm 0.011\%$  and  $0.023 \pm 0.012$  to  $0.049 \pm 0.016\%$  of the OM, respectively (Table  
240 S4). In NC forest smoldering-phase samples,  $C_6H_5NO_4$  has the highest mass contribution (NS1  
241  $0.024 \pm 0.0098\%$ , NS2  $0.010 \pm 0.0027\%$ ), followed by  $C_7H_7NO_4$  (NS1  $0.0087 \pm 0.0030\%$ , NS2  
242  $0.0043 \pm 0.0010\%$ ) and  $C_9H_9NO_4$  (NS1  $0.0052 \pm 0.0033\%$ , NS2  $0.0047 \pm 0.0013\%$ ) (Table S4).  
243 The  $C_6H_5NO_4$  was identified as 4-nitrocatechol by comparing its MS/MS spectrum (Fig. S2b)  
244 with that of an authentic standard (Fig. S3b). The EIC of  $C_9H_9NO_4$  exhibited 3–4 isomers (Fig.  
245 S1i), while only two MS/MS spectra (Fig. S2l,m) were obtained due to the weak EIC intensity  
246 for compounds eluting at times  $\geq 10$  min. The fragmentation patterns of  $C_9H_9NO_4$  compounds  
247 (Fig. S2l,m) are different from that of 2,5-dimethyl-4-nitrobenzoic acid (reference standards with  
248 the same formula, Fig. S3g) without the loss of  $CO_2$ , suggesting that the  $C_9H_9NO_4$  compounds  
249 identified in this work lack a carboxylic acid group. Both MS/MS spectra of  $C_9H_9NO_4$  reflect the  
250 loss of CNO (Fig. S2l,m), suggesting a skeleton of benzisoxazole or benzoxazole. One less likely  
251 explanation for the loss of CNO is the existence of a cyanate ( $-O-C\equiv N$ ) or isocyanate ( $-N=C=O$ )  
252 group, which may not survive the extraction process. Authentic standards are needed to validate  
253 the structure of NAC formulas proposed here.

254            $C_6H_5NO_3$  (Fig. S2a) is identified as 4-nitrophenol using an authentic standard (Fig. S3a).  
255  $C_7H_7NO_4$  has at least two isomers as shown in Fig. S1c that are identified as 4-methyl-5-  
256 nitrocatechol and 3-methyl-6-nitrocatechol according to Iinuma et al. (2010) and Xie et al.  
257 (2017a). Referring to the MS/MS spectrum of 4-nitrocatechol (Fig. S3b), the  $C_6H_5NO_5$   
258 compound should have a nitrocatechol skeleton with an extra hydroxyl group on the benzene  
259 ring. Like  $C_9H_9NO_4$  (Fig. S2l,m), the loss of  $CO_2$  was not observed for the fragmentation of



260  $C_8H_7NO_4$  in the MS/MS spectra (Fig. S2f,g), and a structure with a benzoxazole skeleton was  
261 proposed (Table S2). The  $C_8H_9NO_4$  identified in this work should have several isomers (Fig.  
262 S1f), and two representative MS/MS spectra are provided in Fig. S2h and i. The first isomer of  
263  $C_8H_9NO_4$  has a dominant ion of  $m/z$  137, reflecting the loss of NO and  $CH_3$ . So, the first  
264  $C_8H_9NO_4$  isomer might contain a methyl nitrophenol skeleton with a methoxyl group. The  
265 fragmentation pattern of the second isomer of  $C_8H_9NO_4$  is similar as  $C_7H_7NO_4$ , and the molecule  
266 is postulated as ethyl nitrocatechol.  $C_7H_7NO_5$  has a similar fragmentation pattern as  $C_6H_5NO_4$   
267 and  $C_7H_7NO_4$ , and is identified as methoxyl nitrocatechol. For NC forest burns,  $C_{10}H_7NO_3$  was  
268 only detected in flaming-phase samples (Fig. 1). The MS/MS spectrum of  $C_{10}H_7NO_3$  is subject to  
269 considerable noise, although the loss of  $NO_2$  could be identified (Fig. S2k). The  $C_8H_9NO_5$   
270 compound was identified as dimethoxyl nitrophenol based on its MS/MS spectrum (loss of two  
271  $CH_3$ ). The MS/MS spectra of  $C_{10}H_{11}NO_4$ ,  $C_{10}H_{11}NO_5$ ,  $C_{11}H_{13}NO_5$ , and  $C_{11}H_{13}NO_6$  are very  
272 different from 4-nitrophenol and 4-nitrocatechol (Fig. S3a,b), with multiple losses of  $CH_3$  groups  
273 (Fig. S2o–t). Their structures are proposed in Table S2 and most of these might have at least one  
274 methoxyl group; the loss of CNO might suggest a skeleton of benzisoxazole or benzoxazole.

275 In this work, some of the identified NACs, such as 4-nitrophenol, 4-nitrocatechol, and  
276 methyl nitrocatechols, were commonly observed in BB emissions or BB impacted atmospheres  
277 (Claeys et al., 2014; Mohr et al., 2013; Budisulistiorini et al., 2017). However, these compounds  
278 can also be generated from the photo-oxidation of aromatic VOCs in the presence of  $NO_x$   
279 (Iinuma et al., 2010; Lin et al., 2015; Xie et al., 2017a). Both BB and fossil fuel combustion can  
280 emit a mixture of aromatic precursors (e.g., benzene, toluene) for secondary NACs formation  
281 (Martins et al., 2006; Lewis et al., 2013; George et al., 2014; Gilman et al., 2015; Hatch et al.,  
282 2015; George et al., 2015). Therefore, the NACs uniquely related to BB need to be identified to



283 represent BB BrC. In this work, the NACs formula with molecular weight (MW) < 200 Da (from  
284 C<sub>6</sub>H<sub>5</sub>NO<sub>3</sub>, 138 Da to C<sub>8</sub>H<sub>9</sub>NO<sub>5</sub>, 198 Da) were all identified in secondary organic aerosol (SOA)  
285 generated from chamber reactions with NO<sub>x</sub> (Xie et al., 2017a), although they might have  
286 different structures. The C<sub>10</sub>H<sub>11</sub>NO<sub>4</sub>, C<sub>10</sub>H<sub>11</sub>NO<sub>5</sub>, C<sub>11</sub>H<sub>13</sub>NO<sub>5</sub>, and C<sub>11</sub>H<sub>13</sub>NO<sub>6</sub> compounds  
287 identified in this work were not observed in any previous SOA formation study, to our  
288 knowledge. Among the four formulas, C<sub>10</sub>H<sub>11</sub>NO<sub>4</sub> and C<sub>11</sub>H<sub>13</sub>NO<sub>5</sub> were detected in all samples  
289 with relative mass contributions to OM ranging from 0.0019 ± 0.0008% to 0.014 ± 0.0036% and  
290 0.0016 ± 0.0003% to 0.012 ± 0.0060%, respectively (Table S4). These compounds may contain a  
291 methoxyphenol structure, which is a feature in polar organic compounds from BB (Schauer et al.,  
292 2001; Simpson et al., 2005; Mazzoleni et al., 2007). Before using the C<sub>10</sub>H<sub>11</sub>NO<sub>4</sub>, C<sub>10</sub>H<sub>11</sub>NO<sub>5</sub>,  
293 C<sub>11</sub>H<sub>13</sub>NO<sub>5</sub>, and C<sub>11</sub>H<sub>13</sub>NO<sub>6</sub> compounds as source markers to represent BB BrC chromophores,  
294 additional work is warranted to understand their exact structures and lifetimes in the atmosphere.  
295 The quantification of these compounds might also be subject to high variability due to the usage  
296 of surrogates.

297 **3.3 Contribution of NACs to Abs<sub>365</sub>.** For each sample extract, individual NACs contributions to  
298 Abs<sub>365</sub> (Abs<sub>365,NAC</sub>%) were calculated using their mass concentrations (ng m<sup>-3</sup>) and the MAC<sub>365</sub>  
299 values of individual compound standards (MAC<sub>365,NAC</sub>), as applied in Zhang et al. (2013) and  
300 Xie et al. (2017a). Here, the MAC<sub>365,NAC</sub> value is OM based with a unit of m<sup>2</sup> g<sup>-1</sup>. Each NAC  
301 formula was assigned to an authentic or surrogate standard compound to estimate the  
302 contribution to Abs<sub>365</sub> of extracted OM (Table S2). The UV-Vis spectra of standard compounds  
303 and details of the method for Abs<sub>365,NAC</sub>% calculation are provided in Xie et al. (2017a). The  
304 MAC<sub>365,NAC</sub> values for identified NACs formulas in this work are also obtained from Xie et al.  
305 (2017a) and shown in Table S5. Since the standard compounds used in this work have no



306 absorption at 550 nm, the identified NACs contributions to  $Abs_{550}$  were expected to be 0. The  
307 average and ranges of  $Abs_{365,NAC}\%$  in BB samples are listed in Table S6. For simplicity, the  
308 average  $Abs_{365,NAC}\%$  in the five groups of BB samples (FF, NF1 and 2, NS1 and 2) are stacked  
309 in Fig. 2.

310 In general, the average contributions of total NACs to  $Abs_{365}$  ( $Abs_{365,tNAC}\%$   $0.12 \pm 0.047$   
311 to  $2.44 \pm 0.67\%$ ) are 5–10 times higher than their average  $tNAC_{OM}\%$  ( $0.023 \pm 0.0089$  to  $0.18 \pm$   
312  $0.067\%$ ) in BB samples (Tables S6 and S4), indicating that the identified NACs are strong BrC  
313 chromophores. Similar to the NACs mass contributions and compositions, the samples collected  
314 during flaming periods (NF1 and NF2) have significantly higher ( $p < 0.05$ ) average  $Abs_{365,tNAC}\%$   
315 (NF1  $2.44 \pm 0.67\%$ , NF2  $0.80 \pm 0.23\%$ ) than those collected during smoldering periods (NS1  
316  $1.00 \pm 0.40\%$ , NS2  $0.12 \pm 0.047\%$ ).  $C_6H_5NO_4$  ( $0.098 \pm 0.034$  to  $0.31 \pm 0.11\%$ ) and  $C_9H_9NO_4$   
317 ( $0.21 \pm 0.041$  to  $0.79 \pm 0.14\%$ ) have the highest  $Abs_{365,NAC}\%$  in the FL forest and NC forest  
318 flaming-phase samples.  $C_6H_5NO_4$  has the highest  $Abs_{365,NAC}\%$  (NS1  $0.29 \pm 0.095\%$ , NS2  $0.037$   
319  $\pm 0.0080\%$ ) in the NC forest smoldering-phase samples (Table S6). The average  $Abs_{365,tNAC}\%$   
320 values here are comparable to those obtained for atmospheric particles in Germany ( $0.10 \pm 0.06$   
321 to  $1.13 \pm 1.03\%$ ) (Teich et al., 2017) and Detling, United Kingdom ( $4 \pm 2\%$ ) (Mohr et al., 2013),  
322 but more than 10 times lower than those from chamber reactions of benzene ( $28.0 \pm 8.86\%$ ),  
323 naphthalene ( $20.3 \pm 8.01\%$ ) and *m*-cresol ( $50.5 \pm 15.8\%$ ) with  $NO_x$  (Xie et al., 2017a). Di  
324 Lorenzo et al. (2017) studied the absorbance as a function of molecular size of organic aerosols  
325 from BB, and concluded that the majority of aqueous extracts absorption ( $\lambda = 300$  nm) was due  
326 to compounds with MW greater than 500 Da and carbon number greater than 20. In this work,  
327 less than 5% of the BrC absorption in BB aerosols at  $\lambda = 365$  was ascribed to the identified  
328 NACs with a MW range of 138 to 254 Da, of which the contribution at longer wavelength ( $\lambda =$



329 550 nm) was expected to be 0. Future work is needed to identify high MW light-absorbing  
330 compounds in BB aerosols to apportion a greater fraction of BrC absorption in BB aerosols.

331 **3.4 Regression analysis with EC/OC ratio.** As mentioned earlier, burn conditions are an  
332 important factor impacting the light absorption of BB OC, and the EC/OC ratio has been used as  
333 a measurement proxy of burn conditions to parameterize light-absorbing properties of BB OC in  
334 a number of studies (McMeeking et al., 2014; Saleh et al., 2014; Lu et al., 2015; Pokhrel et al.,  
335 2016; Xie et al., 2017b). We combined the sample measurements from all three BB experiments  
336 and analyzed the correlations of bulk  $MAC_{365}$  vs. EC/OC,  $tNAC_{OM}\%$  vs. EC/OC, and  $Abs_{365,tNAC}\%$   
337 vs. EC/OC (Fig. 3). For the analysis, we removed one FL forest experiment sample due to the  
338 extremely high EC/OC ratio of 0.58 (burn 3, Table S1). Generally, EC/OC ratios are  $< 0.4$  for  
339 laboratory BB (Akagi et al., 2011; Pokhrel et al., 2016; Xie et al., 2017b), and  $\leq 0.1$  for field BB  
340 (Aurell et al., 2015; Xie et al., 2017b; Zhou et al., 2017). Thus, the burn condition of the FL forest  
341 burn 3 (Table S1) is unrepresentative of laboratory BB simulations or field BB.

342 In Fig. 3a, the bulk  $MAC_{365}$  of methanol-extracted OC correlated significantly ( $p < 0.05$ )  
343 with EC/OC for each BB experiment. However, grouping these sample measurements resulted in  
344 no relationship between  $MAC_{365}$  and EC/OC ratio (Fig. 3b). So besides burn conditions, BB BrC  
345 absorption might also be sensitive to fuel type and ambient conditions. Similar results were also  
346 observed for  $MAC_{550}$  vs. EC/OC and  $\mathring{A}_{abs}$  vs. EC/OC correlations (Fig. S4a–d). Unlike the bulk  
347  $MAC_{365}$  and  $MAC_{550}$ ,  $tNAC_{OM}\%$  and  $Abs_{365,tNAC}\%$  correlated ( $p < 0.05$ ) with EC/OC for both  
348 test specific data (Fig. S4e,f) and the pooled experimental data (Fig. 3c,d), supporting that burn  
349 conditions are an important factor in determining NACs formation in BB.

#### 350 **4 Conclusions**



351 The comparisons of light-absorbing properties ( $MAC_{365}$ ,  $MAC_{550}$ , and  $\hat{A}_{abs}$ ) of BB OC  
352 with EC/OC in this study support that burn conditions are not the only factor impacting BrC  
353 absorption (Xie et al., 2017b). Other factors like fuel type and ambient conditions may also play  
354 important roles in determining BrC absorption from BB. It may be impractical to predict BrC  
355 absorption solely based on EC/OC ratios in BB emissions from different fuels or over different  
356 seasons. The present study identified fourteen NAC chemical formulas in BB aerosols. The  
357 average  $tNAC_{OM}\%$  of the FL forest, NC forest 1 and 2 (flaming and smoldering samples were  
358 combined) experiments are  $0.13 \pm 0.059\%$ ,  $0.13 \pm 0.067\%$ , and  $0.11 \pm 0.017\%$ , respectively, and  
359 the NAC composition is also similar across the three BB experiments. The average  $tNAC_{OM}\%$  of  
360 the flaming-phase samples (NF1  $0.18 \pm 0.067\%$ , NF2  $0.16 \pm 0.045\%$ ) is significantly higher ( $p <$   
361  $0.05$ ) than those of smoldering-phase samples (NS1  $0.055 \pm 0.026\%$ , NS2  $0.023 \pm 0.0089\%$ ) in  
362 the two NC forest BB experiments. These results suggest that the formation of NACs from BB  
363 depends on burn conditions, and is less impacted by other factors like fuel type and ambient  
364 conditions. Four of the identified NAC formulas ( $C_{10}H_{11}NO_4$ ,  $C_{10}H_{11}NO_5$ ,  $C_{11}H_{13}NO_5$  and  
365  $C_{11}H_{13}NO_6$ ) were not observed in previous chamber studies examining SOA formation. MS/MS  
366 spectra indicated that these compounds might contain a methoxyphenol skeleton, which is  
367 featured in polar organic compounds from BB. So, these compounds may be uniquely related to  
368 BB and used as source tracers representative of BB-specific BrC in the atmosphere. However,  
369 determinations of their exact structures and lifetimes require further study. The NACs identified  
370 here are strong BrC chromophores, as their total contributions ( $0.12 \pm 0.047$  to  $2.44 \pm 0.67\%$ ) to  
371 bulk  $Ab_{S_{365}}$  are 5–10 times higher than their contributions to OM mass ( $0.023 \pm 0.0089$  to  $0.18 \pm$   
372  $0.067\%$ ). However, more light-absorbing compounds from BB with high MW need to be  
373 identified to apportion the unknown fraction ( $> 95\%$ ) of BrC absorption. Significant correlations





374 ( $p < 0.05$ ) were observed for  $tNAC_{OM}\%$  vs. EC/OC and  $Abs_{365,tNAC}\%$  vs. EC/OC with pooled test  
375 data, supporting that the burn conditions are an important factor for NACs formation in BB.

376

### 377 **Competing interests**

378 The authors declare that they have no conflict of interest.

### 379 **Disclaimer**

380 The views expressed in this article are those of the authors and do not necessarily represent the  
381 views or policies of the U.S. Environmental Protection Agency.

### 382 **Author contribution**

383 MX and AH designed the research. MX and XC performed the experiments. AH and MH  
384 managed sample collection. MX analyzed the data and wrote the paper with significant  
385 contributions from all co-authors.

### 386 **Acknowledgements**

387 This research was supported by the National Natural Science Foundation of China (NSFC,  
388 41701551), the State Key Laboratory of Pollution Control and Resource Reuse Foundation (No.  
389 PCRRF17040), and the Startup Foundation for Introducing Talent of NUIST (No.  
390 2243141801001). We would like to acknowledge Brian Gullett, Johanna Aurell, and Brannon  
391 Seay for assistance with laboratory biomass burning sampling. This work was funded by the U.S.  
392 Environmental Protection Agency. Data used in the writing of this manuscript is available at the  
393 U.S. Environmental Protection Agency's Environmental Dataset Gateway (<https://edg.epa.gov>).

394

### 395 **References**

396 Akagi, S. K., Yokelson, R. J., Wiedinmyer, C., Alvarado, M. J., Reid, J. S., Karl, T., Crounse, J. D., and Wennberg,  
397 P. O.: Emission factors for open and domestic biomass burning for use in atmospheric models, Atmos. Chem.  
398 Phys., 11, 4039-4072, 10.5194/acp-11-4039-2011, 2011.



- 399 Anderson, T. L., Charlson, R. J., Schwartz, S. E., Knutti, R., Boucher, O., Rodhe, H., and Heintzenberg, J.: Climate  
400 forcing by aerosols—a hazy picture, *Science*, 300, 1103–1104, 10.1126/science.1084777, 2003.
- 401 Aurell, J., and Gullett, B. K.: Emission factors from aerial and ground measurements of field and laboratory forest  
402 burns in the southeastern U.S.: PM<sub>2.5</sub>, black and brown carbon, VOC, and PCDD/PCDF, *Environ. Sci.*  
403 *Technol.*, 47, 8443–8452, 10.1021/es402101k, 2013.
- 404 Aurell, J., Gullett, B. K., and Tabor, D.: Emissions from southeastern U.S. grasslands and pine savannas:  
405 comparison of aerial and ground field measurements with laboratory burns, *Atmos. Environ.*, 111, 170–178,  
406 <http://dx.doi.org/10.1016/j.atmosenv.2015.03.001>, 2015.
- 407 Bond, T. C.: Spectral dependence of visible light absorption by carbonaceous particles emitted from coal  
408 combustion, *Geophys. Res. Lett.*, 28, 4075–4078, 10.1029/2001gl013652, 2001.
- 409 Bond, T. C., Streets, D. G., Yarber, K. F., Nelson, S. M., Woo, J.-H., and Klimont, Z.: A technology-based global  
410 inventory of black and organic carbon emissions from combustion, *J. Geophys. Res.*, 109, D14,  
411 10.1029/2003jd003697, 2004.
- 412 Bond, T. C., and Bergstrom, R. W.: Light absorption by carbonaceous particles: an investigative review, *Aerosol Sci.*  
413 *Tech.*, 40, 27–67, 10.1080/02786820500421521, 2006.
- 414 Bond, T. C., Doherty, S. J., Fahey, D. W., Forster, P. M., Berntsen, T., DeAngelo, B. J., Flanner, M. G., Ghan, S.,  
415 Kärcher, B., Koch, D., Kinne, S., Kondo, Y., Quinn, P. K., Sarofim, M. C., Schultz, M. G., Schulz, M.,  
416 Venkataraman, C., Zhang, H., Zhang, S., Bellouin, N., Guttikunda, S. K., Hopke, P. K., Jacobson, M. Z., Kaiser,  
417 J. W., Klimont, Z., Lohmann, U., Schwarz, J. P., Shindell, D., Storelvmo, T., Warren, S. G., and Zender, C. S.:  
418 Bounding the role of black carbon in the climate system: A scientific assessment, *J. Geophys. Res.*, 118, 5380–  
419 5552, 10.1002/jgrd.50171, 2013.
- 420 Budisulistiorini, S. H., Riva, M., Williams, M., Chen, J., Itoh, M., Surratt, J. D., and Kuwata, M.: Light-absorbing  
421 brown carbon aerosol constituents from combustion of Indonesian peat and biomass, *Environ. Sci. Technol.*, 51,  
422 4415–4423, 10.1021/acs.est.7b00397, 2017.
- 423 Chakrabarty, R. K., Gyawali, M., Yatavelli, R. L. N., Pandey, A., Watts, A. C., Knue, J., Chen, L. W. A., Pattison, R.,  
424 R., Tsiabart, A., Samburova, V., and Moosmüller, H.: Brown carbon aerosols from burning of boreal peatlands:  
425 microphysical properties, emission factors, and implications for direct radiative forcing, *Atmos. Chem. Phys.*,  
426 16, 3033–3040, 10.5194/acp-16-3033-2016, 2016.
- 427 Chen, Y., Sheng, G., Bi, X., Feng, Y., Mai, B., and Fu, J.: Emission factors for carbonaceous particles and  
428 polycyclic aromatic hydrocarbons from residential coal combustion in China, *Environ. Sci. Technol.*, 39, 1861–  
429 1867, 10.1021/es0493650, 2005.
- 430 Chen, Y., and Bond, T. C.: Light absorption by organic carbon from wood combustion, *Atmos. Chem. Phys.*, 10,  
431 1773–1787, 10.5194/acp-10-1773-2010, 2010.
- 432 Chow, K. S., Huang, X. H., and Yu, J. Z.: Quantification of nitroaromatic compounds in atmospheric fine  
433 particulate matter in Hong Kong over 3 years: field measurement evidence for secondary formation derived  
434 from biomass burning emissions, *Environ. Chem.*, 13, 665–673, <https://doi.org/10.1071/EN15174>, 2016.
- 435 Claeys, M., Vermeylen, R., Yasmeen, F., Gómez-González, Y., Chi, X., Maenhaut, W., Mészáros, T., and Salma, I.:  
436 Chemical characterisation of humic-like substances from urban, rural and tropical biomass burning  
437 environments using liquid chromatography with UV/vis photodiode array detection and electrospray ionisation  
438 mass spectrometry, *Environ. Chem.*, 9, 273–284, <https://doi.org/10.1071/EN11163>, 2012.
- 439 Desyaterik, Y., Sun, Y., Shen, X., Lee, T., Wang, X., Wang, T., and Collett, J. L.: Speciation of “brown” carbon in  
440 cloud water impacted by agricultural biomass burning in eastern China, *J. Geophys. Res.*, 118, 7389–7399,  
441 10.1002/jgrd.50561, 2013.
- 442 Di Lorenzo, R. A., Washenfelder, R. A., Attwood, A. R., Guo, H., Xu, L., Ng, N. L., Weber, R. J., Baumann, K.,  
443 Edgerton, E., and Young, C. J.: Molecular-size-separated brown carbon absorption for biomass-burning aerosol  
444 at multiple field sites, *Environ. Sci. Technol.*, 51, 3128–3137, 10.1021/acs.est.6b06160, 2017.
- 445 Eriksson, A., Nordin, E., Nystrom, R., Pettersson, E., Swietlicki, E., Bergvall, C., Westerholm, R., Boman, C., and  
446 Pagels, J.: Particulate PAH emissions from residential biomass combustion: time-resolved analysis with aerosol  
447 mass spectrometry, *Environ. Sci. Technol.*, 48, 7143–7150, 10.1021/es500486j, 2014.
- 448 George, I. J., Hays, M. D., Snow, R., Faircloth, J., George, B. J., Long, T., and Baldauf, R. W.: Cold temperature  
449 and biodiesel fuel effects on speciated emissions of volatile organic compounds from diesel trucks, *Environ. Sci.*  
450 *Technol.*, 48, 14782–14789, 10.1021/es502949a, 2014.
- 451 George, I. J., Hays, M. D., Herrington, J. S., Preston, W., Snow, R., Faircloth, J., George, B. J., Long, T., and  
452 Baldauf, R. W.: Effects of cold temperature and ethanol content on VOC emissions from light-duty gasoline  
453 vehicles, *Environ. Sci. Technol.*, 49, 13067–13074, 10.1021/acs.est.5b04102, 2015.



- 454 Gilman, J. B., Lerner, B. M., Kuster, W. C., Goldan, P. D., Warneke, C., Veres, P. R., Roberts, J. M., de Gouw, J. A.,  
455 Burling, I. R., and Yokelson, R. J.: Biomass burning emissions and potential air quality impacts of volatile  
456 organic compounds and other trace gases from fuels common in the US, *Atmos. Chem. Phys.*, 15, 13915-13938,  
457 10.5194/acp-15-13915-2015, 2015.
- 458 Grandesso, E., Gullett, B., Touati, A., and Tabor, D.: Effect of moisture, charge size, and chlorine concentration on  
459 PCDD/F emissions from simulated open burning of forest biomass, *Environ. Sci. Technol.*, 45, 3887-3894,  
460 10.1021/es103686t, 2011.
- 461 Hatch, L. E., Luo, W., Pankow, J. F., Yokelson, R. J., Stockwell, C. E., and Barsanti, K.: Identification and  
462 quantification of gaseous organic compounds emitted from biomass burning using two-dimensional gas  
463 chromatography–time-of-flight mass spectrometry, *Atmos. Chem. Phys.*, 15, 1865-1899, 10.5194/acp-15-1865-  
464 2015, 2015.
- 465 Holder, A. L., Hagler, G. S. W., Aurell, J., Hays, M. D., and Gullett, B. K.: Particulate matter and black carbon  
466 optical properties and emission factors from prescribed fires in the southeastern United States, *J. Geophys. Res.*,  
467 121, 3465-3483, 10.1002/2015jd024321, 2016.
- 468 Hosseini, S., Urbanski, S., Dixit, P., Qi, L., Burling, I. R., Yokelson, R. J., Johnson, T. J., Shrivastava, M., Jung, H.,  
469 and Weise, D. R.: Laboratory characterization of PM emissions from combustion of wildland biomass fuels, *J.*  
470 *Geophys. Res.*, 118, 9914-9929, 10.1002/jgrd.50481, 2013.
- 471 Huang, R.-J., Yang, L., Cao, J., Chen, Y., Chen, Q., Li, Y., Duan, J., Zhu, C., Dai, W., Wang, K., Lin, C., Ni, H.,  
472 Corbin, J. C., Wu, Y., Zhang, R., Tie, X., Hoffmann, T., O’Dowd, C., and Dusek, U.: Brown carbon aerosol in  
473 urban Xi’an, Northwest China: the composition and light absorption properties, *Environ. Sci. Technol.*, 52,  
474 6825-6833, 10.1021/acs.est.8b02386, 2018.
- 475 Inuma, Y., Böge, O., Gräfe, R., and Herrmann, H.: Methyl-nitrocatechols: atmospheric tracer compounds for  
476 biomass burning secondary organic aerosols, *Environ. Sci. Technol.*, 44, 8453-8459, 10.1021/es102938a, 2010.
- 477 Kirchstetter, T. W., Novakov, T., and Hobbs, P. V.: Evidence that the spectral dependence of light absorption by  
478 aerosols is affected by organic carbon, *J. Geophys. Res.*, 109, D21208, 10.1029/2004jd004999, 2004.
- 479 Lack, D. A., and Langridge, J. M.: On the attribution of black and brown carbon light absorption using the  
480 Ångström exponent, *Atmos. Chem. Phys.*, 13, 10535-10543, 10.5194/acp-13-10535-2013, 2013.
- 481 Laskin, A., Laskin, J., and Nizkorodov, S. A.: Chemistry of atmospheric brown carbon, *Chem. Rev.*, 115, 4335-  
482 4382, 10.1021/cr5006167, 2015.
- 483 Lewis, A. C., Evans, M. J., Hopkins, J. R., Punjabi, S., Read, K. A., Purvis, R. M., Andrews, S. J., Moller, S. J.,  
484 Carpenter, L. J., Lee, J. D., Rickard, A. R., Palmer, P. I., and Parrington, M.: The influence of biomass burning  
485 on the global distribution of selected non-methane organic compounds, *Atmos. Chem. Phys.*, 13, 851-867,  
486 10.5194/acp-13-851-2013, 2013.
- 487 Lin, P., Liu, J. M., Shilling, J. E., Kathmann, S. M., Laskin, J., and Laskin, A.: Molecular characterization of brown  
488 carbon (BrC) chromophores in secondary organic aerosol generated from photo-oxidation of toluene, *Phys.*  
489 *Chem. Chem. Phys.*, 17, 23312-23325, 10.1039/c5cp02563j, 2015.
- 490 Lin, P., Aiona, P. K., Li, Y., Shiraiwa, M., Laskin, J., Nizkorodov, S. A., and Laskin, A.: Molecular characterization  
491 of brown carbon in biomass burning aerosol particles, *Environ. Sci. Technol.*, 50, 11815-11824,  
492 10.1021/acs.est.6b03024, 2016.
- 493 Lin, P., Bluvshstein, N., Rudich, Y., Nizkorodov, S. A., Laskin, J., and Laskin, A.: Molecular chemistry of  
494 atmospheric brown carbon inferred from a nationwide biomass burning event, *Environ. Sci. Technol.*, 51,  
495 11561-11570, 10.1021/acs.est.7b02276, 2017.
- 496 Lin, Y.-H., Budisulistiorini, S. H., Chu, K., Siejack, R. A., Zhang, H., Riva, M., Zhang, Z., Gold, A., Kautzman, K.  
497 E., and Surratt, J. D.: Light-absorbing oligomer formation in secondary organic aerosol from reactive uptake of  
498 isoprene epoxydiols, *Environ. Sci. Technol.*, 48, 12012-12021, 10.1021/es503142b, 2014.
- 499 Lu, Z., Streets, D. G., Winijkul, E., Yan, F., Chen, Y., Bond, T. C., Feng, Y., Dubey, M. K., Liu, S., Pinto, J. P., and  
500 Carmichael, G. R.: Light absorption properties and radiative effects of primary organic aerosol emissions,  
501 *Environ. Sci. Technol.*, 49, 4868-4877, 10.1021/acs.est.5b00211, 2015.
- 502 Martins, L. D., Andrade, M. F., Freitas, E. D., Pretto, A., Gatti, L. V., Albuquerque, É. L., Tomaz, E., Guardani, M.  
503 L., Martins, M. H. R. B., and Junior, O. M. A.: Emission factors for gas-powered vehicles traveling through  
504 road tunnels in São Paulo, Brazil, *Environ. Sci. Technol.*, 40, 6722-6729, 10.1021/es052441u, 2006.
- 505 Martinsson, J., Eriksson, A., Nielsen, I. E., Malmberg, V. B., Ahlberg, E., Andersen, C., Lindgren, R., Nystrom, R.,  
506 Nordin, E., and Brune, W.: Impacts of combustion conditions and photochemical processing on the light  
507 absorption of biomass combustion aerosol, *Environ. Sci. Technol.*, 49, 14663-14671, 10.1021/acs.est.5b03205,  
508 2015.



- 509 Mazzoleni, L. R., Zielinska, B., and Moosmüller, H.: Emissions of levoglucosan, methoxy phenols, and organic  
510 acids from prescribed burns, laboratory combustion of wildland fuels, and residential wood combustion,  
511 *Environ. Sci. Technol.*, 41, 2115-2122, 10.1021/es061702c, 2007.
- 512 McMeeking, G., Fortner, E., Onasch, T., Taylor, J., Flynn, M., Coe, H., and Kreidenweis, S.: Impacts of  
513 nonrefractory material on light absorption by aerosols emitted from biomass burning, *J. Geophys. Res.*, 119,  
514 12,272-212,286, 2014.
- 515 Mohr, C., Lopez-Hilfiker, F. D., Zotter, P., Prévôt, A. S. H., Xu, L., Ng, N. L., Herndon, S. C., Williams, L. R.,  
516 Franklin, J. P., Zahniser, M. S., Worsnop, D. R., Knighton, W. B., Aiken, A. C., Gorkowski, K. J., Dubey, M.  
517 K., Allan, J. D., and Thornton, J. A.: Contribution of nitrated phenols to wood burning brown carbon light  
518 absorption in Detling, United Kingdom during winter time, *Environ. Sci. Technol.*, 47, 6316-6324,  
519 10.1021/es400683v, 2013.
- 520 Nielsen, I. E., Eriksson, A. C., Lindgren, R., Martinsson, J., Nyström, R., Nordin, E. Z., Sadiktsis, I., Boman, C.,  
521 Nøjgaard, J. K., and Pagels, J.: Time-resolved analysis of particle emissions from residential biomass  
522 combustion—Emissions of refractory black carbon, PAHs and organic tracers, *Atmos. Environ.*, 165, 179-190,  
523 2017.
- 524 NIOSH, 1999. National Institute of Occupational Safety and Health. Elemental carbon (diesel particulate): Method  
525 5040, Rep. <https://www.cdc.gov/niosh/docs/2003-154/pdfs/5040f3.pdf> (1999). Accessed March, 2018.
- 526 Pokhrel, R. P., Wagner, N. L., Langridge, J. M., Lack, D. A., Jayarathne, T., Stone, E. A., Stockwell, C. E.,  
527 Yokelson, R. J., and Murphy, S. M.: Parameterization of single-scattering albedo (SSA) and absorption  
528 Ångström exponent (AAE) with EC/OC for aerosol emissions from biomass burning, *Atmos. Chem. Phys.*, 16,  
529 9549-9561, 10.5194/acp-16-9549-2016, 2016.
- 530 Ramanathan, V., Crutzen, P. J., Kiehl, J. T., and Rosenfeld, D.: Aerosols, climate, and the hydrological cycle,  
531 *Science*, 294, 2119-2124, 10.1126/science.1064034, 2001.
- 532 Riddle, S. G., Jakober, C. A., Robert, M. A., Cahill, T. M., Charles, M. J., and Kleeman, M. J.: Large PAHs detected  
533 in fine particulate matter emitted from light-duty gasoline vehicles, *Atmos. Environ.*, 41, 8658-8668,  
534 <https://doi.org/10.1016/j.atmosenv.2007.07.023>, 2007.
- 535 Saleh, R., Robinson, E. S., Tkacik, D. S., Ahern, A. T., Liu, S., Aiken, A. C., Sullivan, R. C., Presto, A. A., Dubey,  
536 M. K., Yokelson, R. J., Donahue, N. M., and Robinson, A. L.: Brownness of organics in aerosols from biomass  
537 burning linked to their black carbon content, *Nature Geosci.*, 7, 647-650, 10.1038/ngeo2220, 2014.
- 538 Samburova, V., Connolly, J., Gyawali, M., Yatavelli, R. L. N., Watts, A. C., Chakrabarty, R. K., Zielinska, B.,  
539 Moosmüller, H., and Khlystov, A.: Polycyclic aromatic hydrocarbons in biomass-burning emissions and their  
540 contribution to light absorption and aerosol toxicity, *Sci. Total Environ.*, 568, 391-401,  
541 <http://doi.org/10.1016/j.scitotenv.2016.06.026>, 2016.
- 542 Schauer, J. J., Kleeman, M. J., Cass, G. R., and Simoneit, B. R. T.: Measurement of emissions from air pollution  
543 sources. 3. C1-C29 organic compounds from fireplace combustion of wood, *Environ. Sci. Technol.*, 35, 1716-  
544 1728, 10.1021/es001331e, 2001.
- 545 Simpson, C. D., Paulsen, M., Dills, R. L., Liu, L. J. S., and Kalman, D. A.: Determination of methoxyphenols in  
546 ambient atmospheric particulate matter: tracers for wood combustion, *Environ. Sci. Technol.*, 39, 631-637,  
547 10.1021/es0486871, 2005.
- 548 Teich, M., van Pinxteren, D., Kecorius, S., Wang, Z., and Herrmann, H.: First quantification of imidazoles in  
549 ambient aerosol particles: potential photosensitizers, brown carbon constituents, and hazardous components,  
550 *Environ. Sci. Technol.*, 50, 1166-1173, 10.1021/acs.est.5b05474, 2016.
- 551 Teich, M., van Pinxteren, D., Wang, M., Kecorius, S., Wang, Z., Müller, T., Močnik, G., and Herrmann, H.:  
552 Contributions of nitrated aromatic compounds to the light absorption of water-soluble and particulate brown  
553 carbon in different atmospheric environments in Germany and China, *Atmos. Chem. Phys.*, 17, 1653-1672,  
554 10.5194/acp-17-1653-2017, 2017.
- 555 Turpin, B. J., and Lim, H.-J.: Species contributions to PM<sub>2.5</sub> mass concentrations: revisiting common assumptions  
556 for estimating organic mass, *Aerosol Sci. Tech.*, 35, 602-610, 10.1080/02786820119445, 2001.
- 557 Xie, M., Chen, X., Hays, M. D., Lewandowski, M., Offenberg, J., Kleindienst, T. E., and Holder, A. L.: Light  
558 absorption of secondary organic aerosol: composition and contribution of nitroaromatic compounds, *Environ.*  
559 *Sci. Technol.*, 51, 11607-11616, 10.1021/acs.est.7b03263, 2017a.
- 560 Xie, M., Hays, M. D., and Holder, A. L.: Light-absorbing organic carbon from prescribed and laboratory biomass  
561 burning and gasoline vehicle emissions, *Sci. Rep.*, 7, 7318, 10.1038/s41598-017-06981-8, 2017b.
- 562 Zhang, X., Lin, Y.-H., Surratt, J. D., and Weber, R. J.: Sources, composition and absorption Ångström exponent of  
563 light-absorbing organic components in aerosol extracts from the Los Angeles Basin, *Environ. Sci. Technol.*, 47,  
564 3685-3693, 10.1021/es305047b, 2013.



565 Zhou, Y., Xing, X., Lang, J., Chen, D., Cheng, S., Wei, L., Wei, X., and Liu, C.: A comprehensive biomass burning  
566 emission inventory with high spatial and temporal resolution in China, Atmos. Chem. Phys., 17, 2839-2864,  
567 10.5194/acp-17-2839-2017, 2017.



**Table 1.** EC/OC ratio, OC extraction efficiency and light-absorbing properties of organic aerosols in PM<sub>2.5</sub> from laboratory biomass burning.

Experiment	Phase	Abbr.	Fuels	EC/OC	Extraction efficiency (%)	MAC <sub>365</sub> (m <sup>2</sup> gC <sup>-1</sup> )	MAC <sub>350</sub> (m <sup>2</sup> gC <sup>-1</sup> )	Aabs
FL forest <sup>a</sup>	No separation	FF	long leaf pine (N=9)	0.21 ± 0.16	97.0 ± 1.87	1.13 ± 0.15	0.053 ± 0.023	7.36 ± 0.59
NC forest 1	Flaming	NF1	hardwood/loblolly pine (N=3)	0.042 ± 0.014	97.7 ± 0.41	1.47 ± 0.25	0.15 ± 0.065	5.68 ± 0.70
	Smoldering	NS1	hardwood/loblolly pine (N=3)	0.0098 ± 0.0024	97.9 ± 0.22	1.00 ± 0.11	0.054 ± 0.015	6.83 ± 0.52
NC forest 2	Flaming	NF2	hardwood/loblolly pine (4)	0.049 ± 0.011	99.5 ± 0.33	4.07 ± 0.15	0.17 ± 0.0051	7.38 ± 0.069
	Smoldering	NS2	hardwood/loblolly pine (4)	0.0075 ± 0.0026	99.2 ± 0.10	3.25 ± 0.35	0.12 ± 0.033	7.95 ± 0.22

<sup>a</sup> Data were obtained from Xie et al. (2017b).

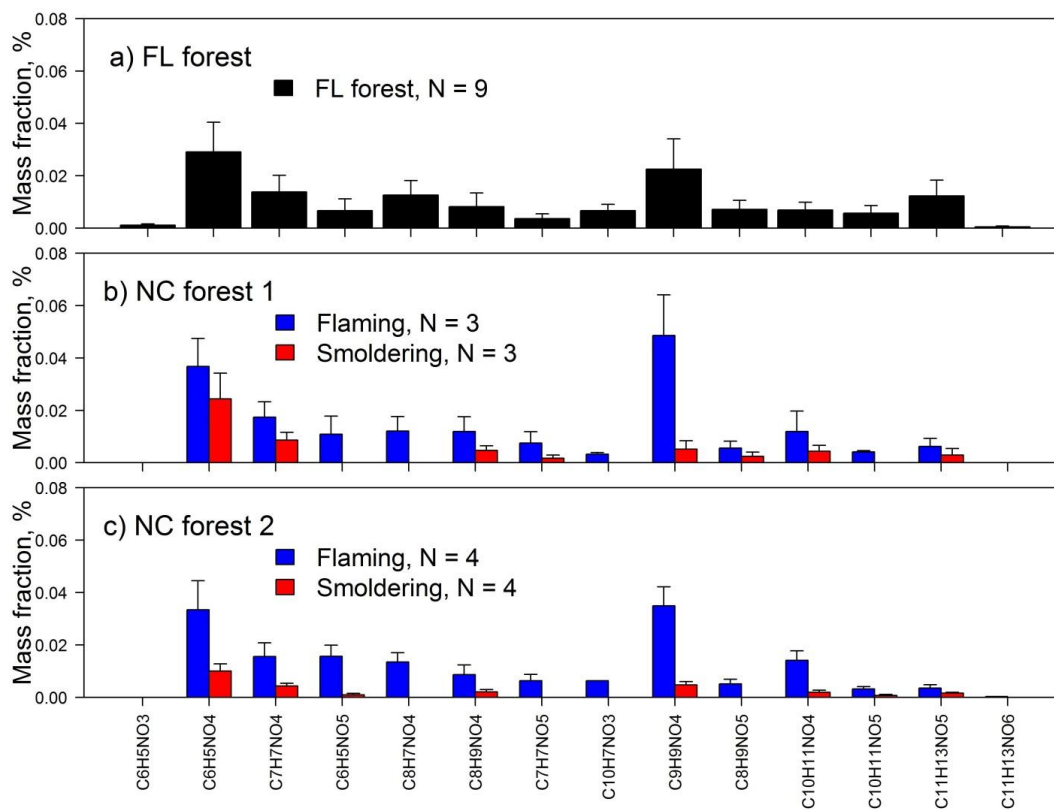


**Figure 1. Relative mass contributions of identified nitroaromatic compounds in BB burning samples collected during (a) FL forest, (b) NC forest 1 and (c) NC forest 2 experiments.**

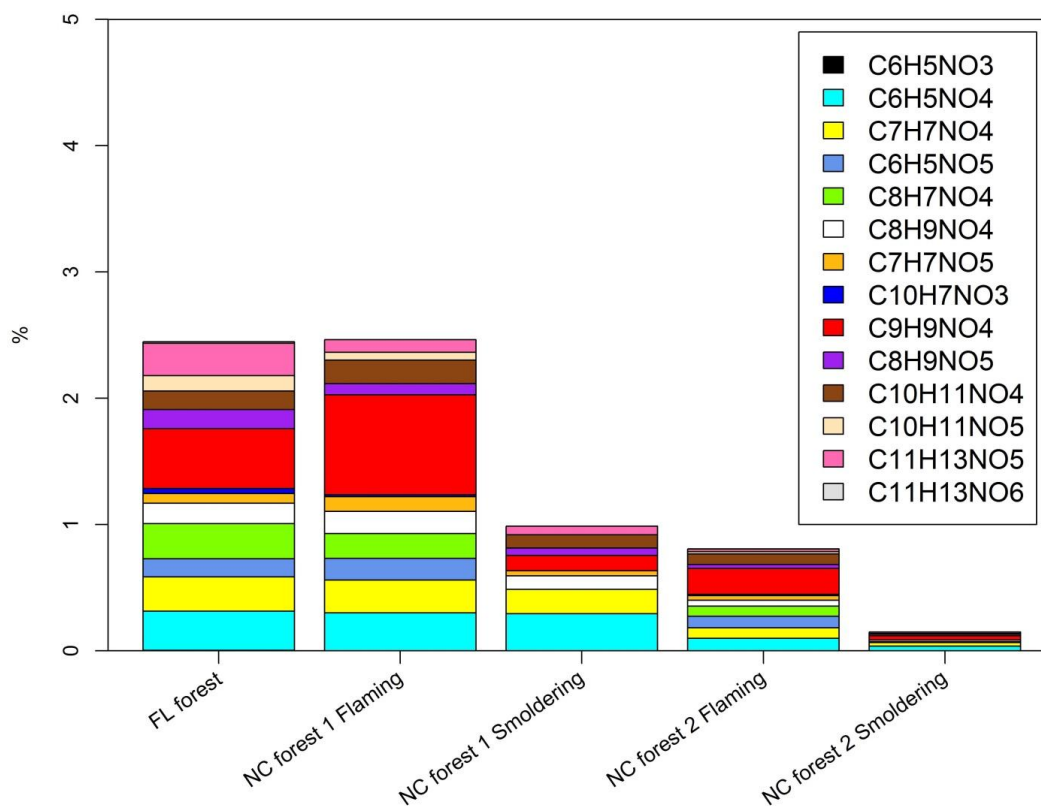


**Figure 2.** Average contributions (%) of nitroaromatic compounds to Abs<sub>365</sub> of methanol extractable OC from laboratory biomass burning.



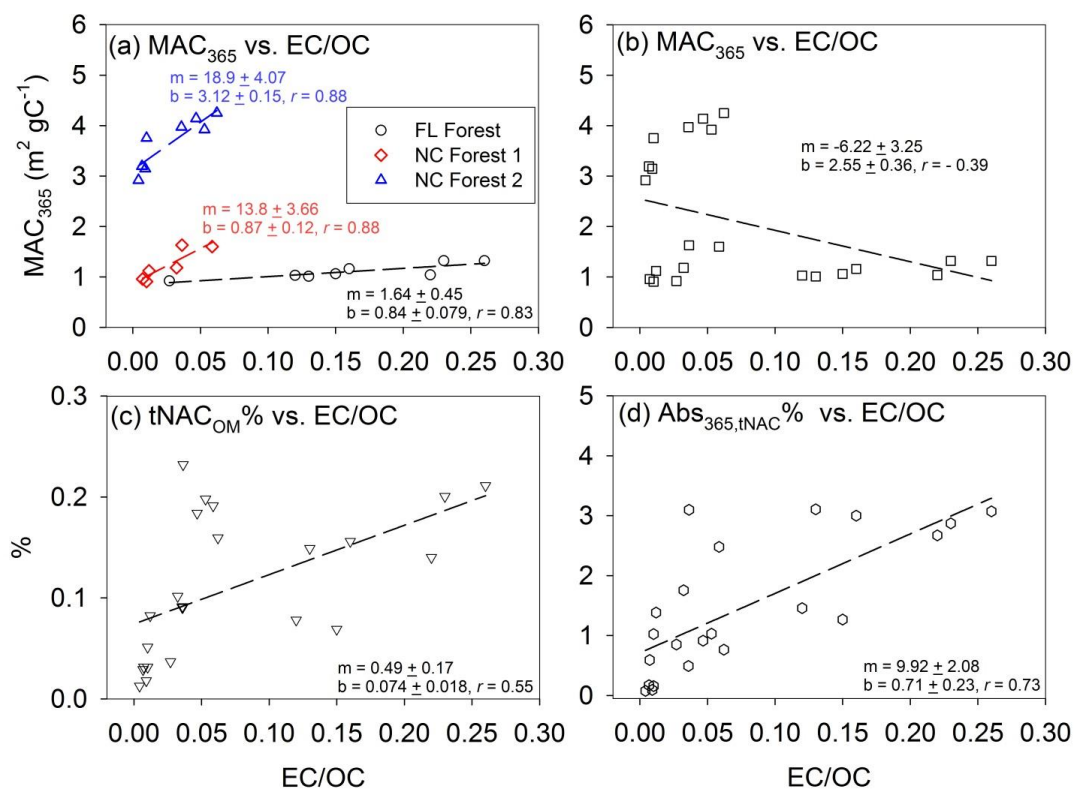


Figure 3. Linear regressions of (a)  $MAC_{365}$  vs. EC/OC with sample data of each experiment, (b)  $MAC_{365}$  vs. EC/OC, (c)  $tNAC_{OM}\%$  vs. EC/OC and (d)  $Abs_{365,tNAC}\%$  vs. EC/OC with pooled sample data of all the three experiments.